Deep-Sea Research, Vol. 28A, No. 11, pp. 1239 to 1264, 1981.
Printed in Great Britain.

0198-0149/81/111239-25 $02.00/0

South Atlantic thermocline ventilation*

ARNOLD L. GORDON†

(*Received* 12 *December* 1980; *in revised form* 23 *March* 1981; *accepted* 19 *April* 1981)

Abstract—South Atlantic Central Water (SACW) is carried poleward within a narrow longitude interval off the Argentine coast by the Brazil Current after confluence with the Malvinas (Falkland) Current. Hydrographic data obtained from the R.V. *Atlantis II* in December 1979 and January 1980 indicate that within the SACW poleward extension, convective processes are important in ventilating the main thermocline to the north. A number of relatively warm, salty intrusions 100 m thick are found within the 12 to 17°C layer of the thermocline along 38°S. These features are about 0.2×10^{-3} more saline than the regional potential temperature–salinity (θ–S) curve of the SACW thermocline and represent local oxygen maxima and nutrient minima. The characteristics of the intrusion are similar to thick remnant winter-mixed layers within various pockets (warm-core eddies) of SACW found further south. The observations support MCCARTNEY's 1977 (*A Voyage of Discovery*, M. Angel, editor, pp. 103–119, Pergamon) suggestion that the Brazil–Malvinas confluence region is the source of a thermostad in the South Atlantic thermocline. The present data suggest that a family of winter altered, relatively salty mixed layers and intrusions are formed in the poleward extension of the SACW thermocline waters, which then spread northward into the main thermocline. The number of family members and their range of θ–S characteristics depend on the distribution of warm eddies and meanders during the winter period. The lower boundary of the intrusions have density ratios ($R = \alpha\Delta T/\beta\Delta S$) of 1.2 to 1.3, making them unstable to salt-finger activity. Salt fingers are likely to be the primary process that integrates the excess salt of the intrusions into a broader, but less extreme positive salinity anomaly (relative to the South Atlantic thermocline T–S curve), which is associated with the 12 to 17°C weak thermostad of the southwest Atlantic. It is suggested that deep winter convective processes within the SACW extension not only transfer salt and oxygen to mid-thermocline depths, but it also induces significant downward salt flux by salt-finger activity at mid-thermocline depths. Similar processes may be important in all poleward edges of the world thermocline, particularly along the western sectors.

1. INTRODUCTION

THE confluence of the poleward flowing South Atlantic Central Water (SACW) within the Brazil Current with the Subantarctic Water carried northward by the Malvinas (Falkland) Current, adjacent to the coast of Argentina, initiates a strong frontal zone (BRENNECKE, 1921). DEACON (1937) called the division between cold and warm water the Subtropical Convergence, while MCCARTNEY (1977) referred to it as the beginning of a nearly circumpolar Subantarctic Front.

The frontal zone induced by the confluence extends southward as far as 49°S (DEACON, 1937) before returning north. In this way it defines a poleward extension of SACW within the rather limited longitudes of 50 to 55°W. The SACW extension is strikingly revealed by satellite infrared (i.r.) images (JOHNSON and NORRIS, 1977; LEGECKIS, 1978; LUTJEHARMS

* Lamont-Doherty Contribution No. 3182.
† Lamont-Doherty Geological Observatory of Columbia University, Palisades, NY 10964, U.S.A.

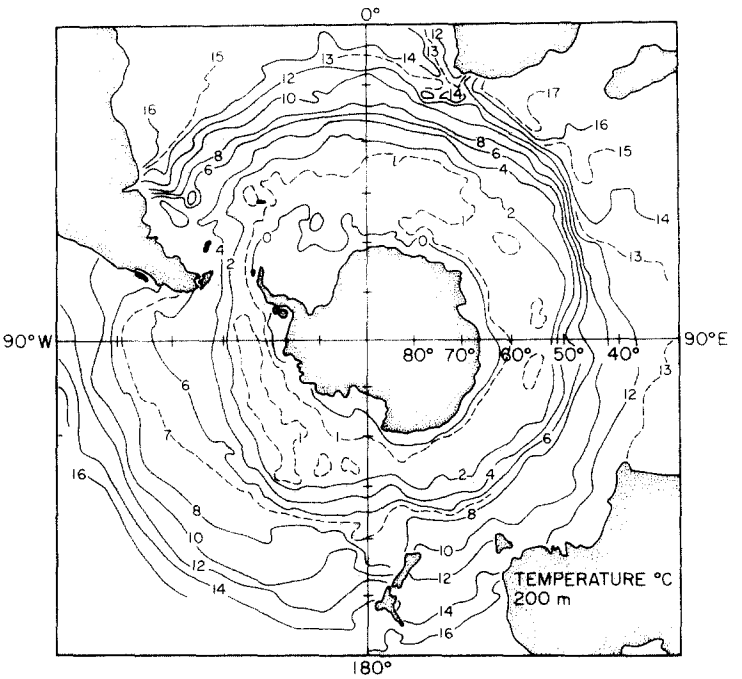

Fig. 2(a).

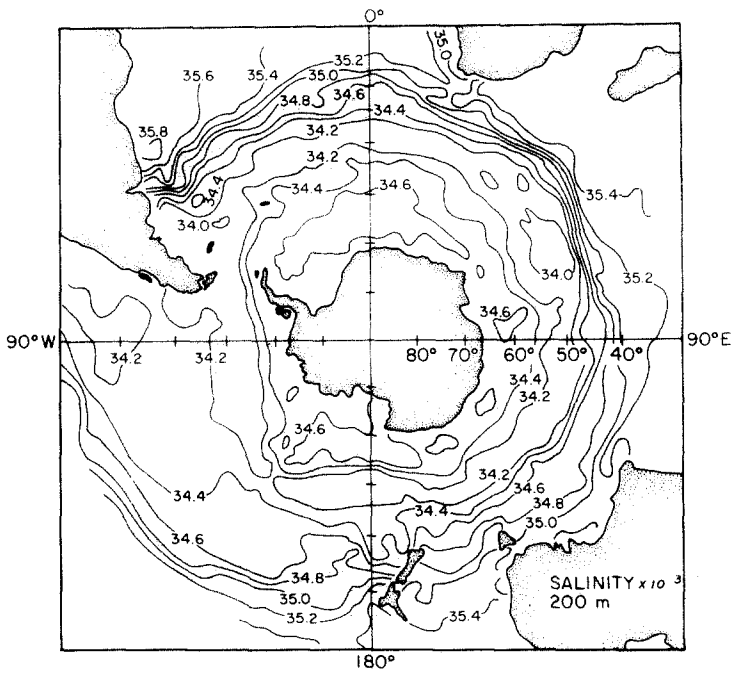

Fig. 2(b).
Caption on p. 1243.

Fig. 1. Satellite i.r. image of the South Atlantic Central Water extension on 1 January 1980. The position of Stas 7 and 37 are shown for reference. The image was supplied by RICHARD LEGECKIS of NOAA.

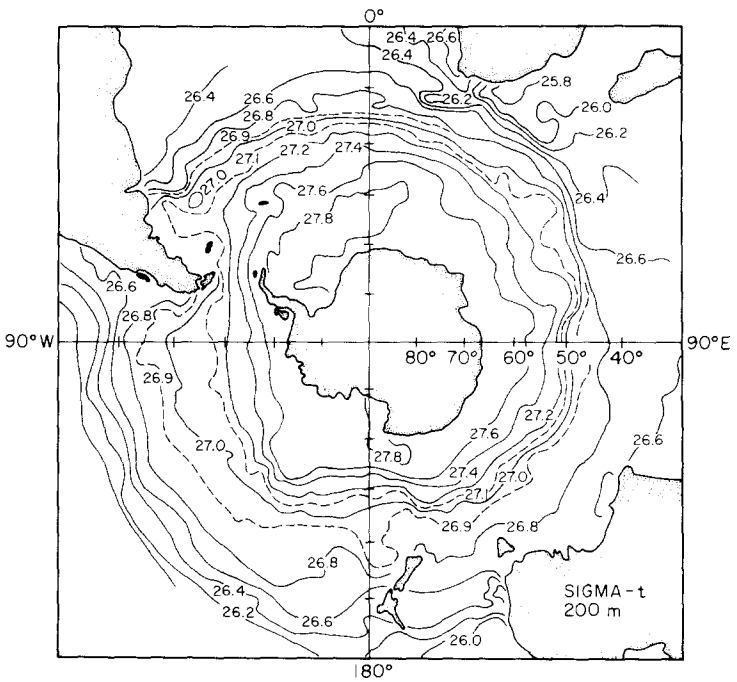

Fig. 2(c).

Fig. 2. Temperature (a), salinity (b), and σ_θ (c) distribution at 200 m south of 30°S. Isopleths are from computer contouring of non-synoptic hydrographic data averaged at 1° latitude by 2° longitude grid points. Figure from GORDON and BAKER (1981). The objective analysis procedure used attentuates structures with scales of less than 300 km, hence the SACW extension appears less well-developed than it does using a synoptic data set.

and BAKER, 1980). JOHNSON and NORRIS (1977), using SKYLAB multi-spectra scanner data of 2 September 1973, found thermal gradients at the confluence of 1°C (250 m)$^{-1}$ with a maximum of 1°C (67 m)$^{-1}$. The satellite images (Fig. 1) show the SACW extension pattern to be variable, being composed of many warm eddies, filiments, and meanders, though the extension in some form is apparently always present and can be considered as a quasi-stationary structure.

Further evidence for a quasi-stationary SACW extension is derived from various atlas presentations, which show a poleward loop in the climatic position of ocean parameter isopleths near 50 to 55°W off the Argentine coast (for example, see the atlas plates in DEFANT, 1961). In the recent Southern Ocean atlas (GORDON and MOLINELLI, 1981; GORDON and BAKER, 1981), the SACW extension, with a meridional amplitude of 350 km, is well established (Fig. 2).

Poleward extension of warm waters is expected to enhance ocean-to-atmosphere heat flux by increasing the contrast of ocean and air temperatures. Bunker's annual heat flux map for the Atlantic Ocean (BUNKER, 1980) shows a localized maximum of ocean heat loss within the SACW extension region of 25 to 50 W m^{-2}.

Dynamic topography charts for the southwest Atlantic (REID, NOWLIN and PATZERT, 1977) show thermohaline SACW extension discussed above associated with an anti-cyclonic circulation pattern. This structure shifts poleward and becomes more restricted in the east–west direction with increasing depth.

A poleward extension of central thermocline water also appears in the climatic chart (Fig. 2) for the other southern hemisphere oceans. In the southwest Indian Ocean the Agulhas Current carries South Indian Central Waters southward and westward along the South Africa coast before abruptly returning eastward (WYRTKI, 1971; LUTJEHARMS and BAKER, 1980). BUNKER (1980) determined the oceanic heat loss associated with the poleward extension of South Indian Ocean thermocline with the Agulhas system to be over 100 W m^{-2}. A less developed warm water extension occurs in the southwest Pacific Ocean adjacent to Australia by the East Australia Current, often in eddy form, as far as the latitude of Tasmania (WYRTKI, 1962; HAMON, 1970) and adjacent to the east coast of New Zealand by the East Auckland and East Cape currents (STANTON, 1973).

The poleward extensions of thermocline waters of the southern hemisphere can be considered as overshoots of the western boundary currents, though in view of sea–air exchange processes, isotherms and isohalines need not exactly parallel the streamlines. Western boundary current poleward loops after separation from the lateral boundary are displayed in numerical model results for wind-driven subtropical gyre circulation when non-linear inertial terms are included. The structure of the overshoot is dependent on the form of the frictional mechanism, particularly at the side walls (POND and BRYAN, 1976).

In the northern hemisphere quasi-stationary poleward extensions of the central thermocline waters are less well developed. The mean annual temperature distribution at 200 m for the North Atlantic (SCHROEDER, 1963) indicates no significant poleward excursion from the general northeast trend of the 15°C isotherm, usually associated with the Gulf Stream axis from Cape Hatteras to 50°W. In addition, inspection of the monthly mean surface temperature and mean Gulf Stream axis compiled by the National Weather Service (Gulf Stream—a monthly summary) reveals no poleward extension in the mean field, though a high degree of activity at the transient level is clearly present. East of 50°W the Gulf Stream branches, with a northern limb, the North Atlantic Current, inducing a warm water feature along 40 to 45°W east of the Grand Banks (ISELIN, 1936). While this feature is analagous to a western boundary current overshoot and poleward extension of thermocline waters, it is far downstream of the initial separation of the western boundary current from the continental margins, and there is controversy regarding the circulation pattern associated with the thermocline water east of the Grand Banks (WORTHINGTON, 1972, 1976; CLARKE, HILL, REINIGER and WARREN, 1980).

The Kuroshio Current east of the Izu-Ogasawara Ridge exhibits a poleward meander between 142 and 145°E (KAWAI, 1972), where it often ejects large warm-core eddies into a complex transition (or perturbed area, KAWAI, 1972) between the Kuroshio and Oyashio frontal zones. The poleward meander is evident on climatic mean charts (KAWAI, 1972; WINTERFELD and STOMMEL, 1972; JAPAN OCEANOGRAPHIC DATA CENTER, 1978).

The primary objective of this paper is to present data showing that thermohaline alterations within the poleward extension of the SACW leads to renewal of mid-depth thermocline characteristics to the north and that this process accelerates salt-finger associated vertical thermohaline flux at mid-thermocline levels.

2. THE DATA

Cruise 107–3 of R.V. *Atlantis II* in December 1979 and January 1980 was directed at the study of the thermohaline structure of the SACW extension (Fig. 3). The data include 96 CTD–O_2 hydrographic stations including water samples from a 24 bottle rosette sampler

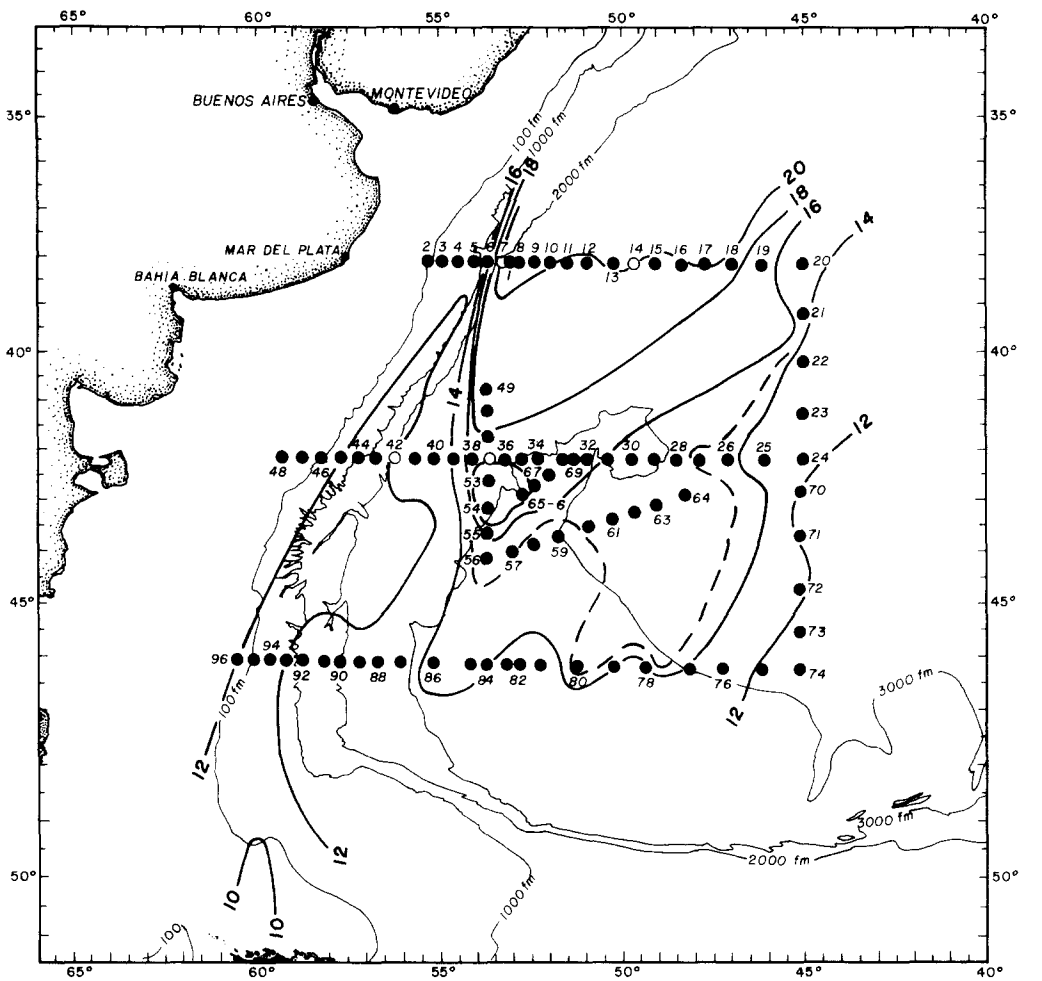

Fig. 3. Distribution of hydrographic stations obtained during R.V. *Atlantis* cruise 107–3, 8 December 1979 to 10 January 1980. The isotherms represent surface temperature as measured along the ship's track; some minor variations are obtained from interpretation of the satellite i.r. images.

for calibration data and nutrient determinations. The cold axis, colder than 12°C, over the continental slope represents advection of Subantarctic Water by the Malvinas (Falkland) Current, which faithfully maintains a fixed position relative to the continental margin until the confluence with the Brazil Current. East of the Malvinas Current the elevated surface water temperatures of the SACW extension are evident, with return to lower temperatures over the 45°W eastern limit of the station array.

3. ZONAL SECTIONS

The temperature, salinity, and oxygen sections for the three primary east–west sections, 38, 42, and 46°S (Fig. 4) reveal the contrasting stratification of the SACW extension with

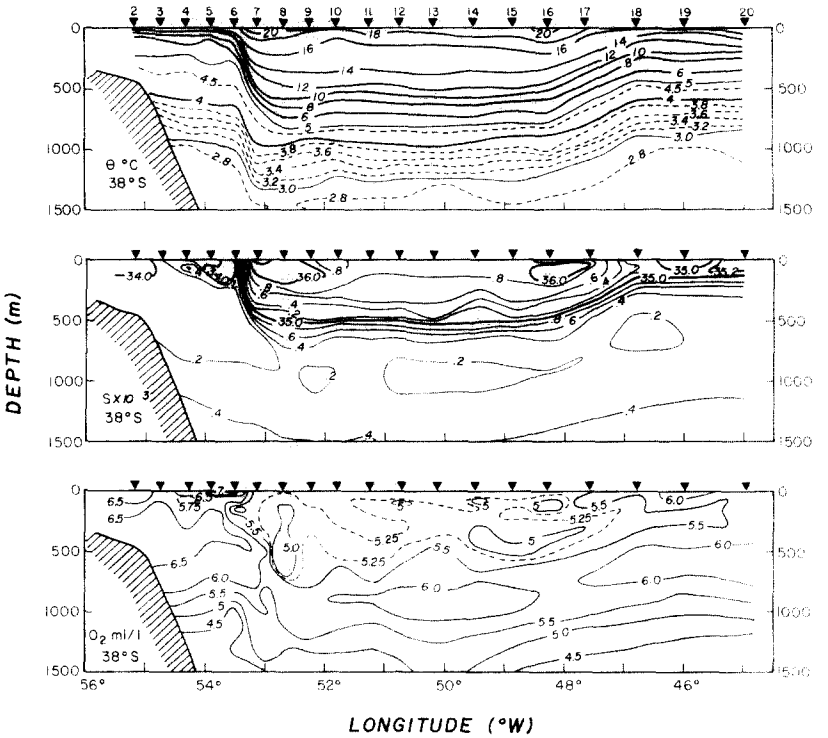
θ °C
38°S
S x 10 3
38°S
O2 ml/l
38°S
DEPTH (m)
LONGITUDE (°W)

Fig. 4(a).

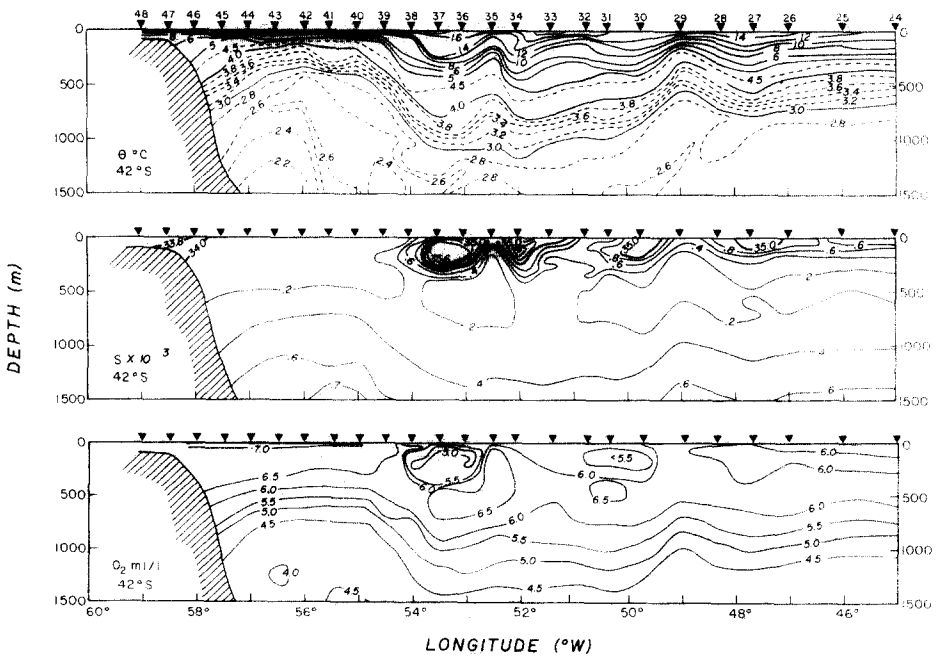
θ °C
42°S
S x 10 3
42°S
O2 ml/l
42°S
DEPTH (m)
LONGITUDE (°W)

Fig. 4(b).

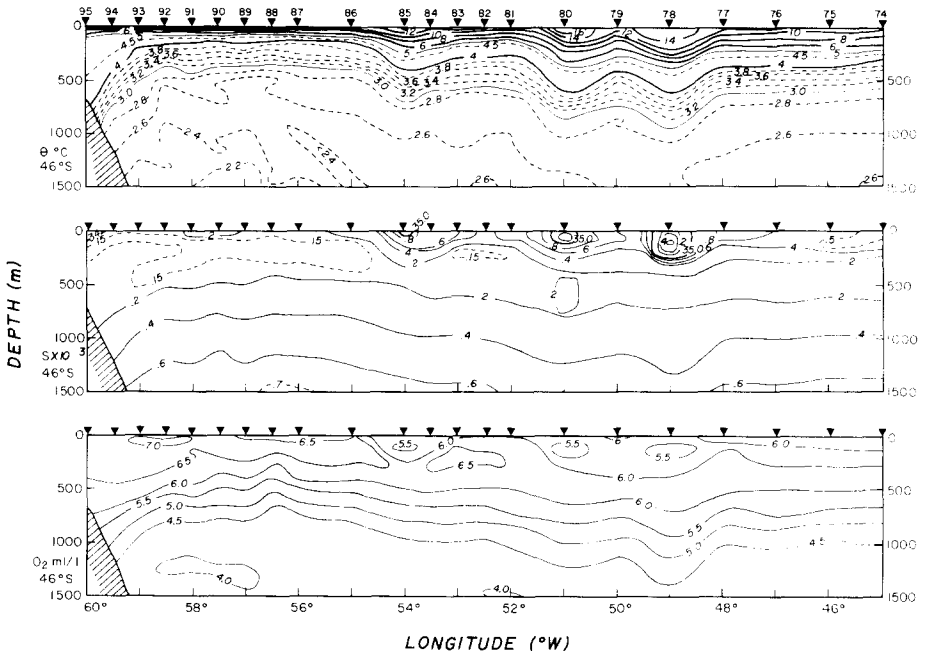

Fig. 4(c).

Fig. 4. Potential temperature, salinity, and oxygen along the three primary zone sections obtained during R.V. *Atlantis* cruise 107 3. (a) Along 38 S. (b) along 42 S. and (c) along 46 S.

the colder Subantarctic Water. At 38°S the isotherms and isohalines deepen between Stas 7 and 17 as the anti-cyclonic baroclinic field of the SACW extension is encountered. The warmest, saltiest water, with the most intense thermocline oxygen minimum, occurs at the edges of the extension (between Stas 7 to 9 and 16 to 17). The ship drift during these stations indicated strong meridional flow consistent with the anti-cyclonic baroclinicity.

The thermocline is strongest at levels below 500 m from the 6 to 12°C isotherms. Above the 12 to 13°C isotherms the vertical gradient is much reduced, increasing again above the 16 to 17°C isotherms. The thermocline weakening within the 12 to 17°C layer is accompanied by a similar weakening in the salinity gradient. As discussed below, the 12 to 17°C layer of the southwest Atlantic is anomalously salty relative to the rest of the South Atlantic thermocline.

McCartney (1977) found reduced vertical temperature gradients ". . . centered around 14°C south of 32°S and somewhat warmer to the north" in the *Hudson*-70 data along 30°W. He also pointed out that *Discovery* Sta. 675 (at 34°S, 30°W) shows reduced gradient near 13.5°C. McCartney (1977) called the low gradient stratum the Subantarctic Mode Water (SAMW), with the variety found in the southwest Atlantic representing the warmest, least dense form.

The lowest oxygen concentration in the thermocline is generally near the 12°C isotherm at the base of the weakened thermocline layer, often with equally low oxygen levels at the top boundary near 18°C.

A broad subthermocline salinity minimum marks the Antarctic Intermediate Water (AAIW). With a salinity near 34.2×10^{-3} and a local oxygen maximum above 6 ml l^{-1}, it

parallels the 4°C isotherm. Over the continental slope there is a thick low-salinity, high-oxygen layer reaching to depths of 800 m. The AAIW characteristics form a continuous feature with a subsurface layer of slope water (approximately from 200 to 800 m), which is presumably carried northward from the subantarctic by the Malvinas Current. This component of the slope water column can be called Malvinas Water. The water mass similarities between the AAIW, Malvinas Water, and Drake Passage isohaline thermocline (MOLINELLI, 1978) waters are discussed in section 4.

Below the low-salinity layer (and the 1500-m cut-off of the zonal sections) are the abyssal water characteristics of North Atlantic Deep Water and Antarctic Bottom Water (WÜST, 1935; REID *et al.*, 1977). The North Atlantic Deep Water characteristic high salinity is surprisingly coherent with the intensity of the thermocline signal, though Antarctic Bottom Water is not coherent. Thus, the poleward extension can be traced to about 3500 m.

Along 42 and 46°S the SACW thermocline is strongly attentuated, forming numerous isolated pockets or warm, saline-core eddies. The best developed is near Stas 36 and 37 along 42°S. This is a region of warmer surface water (Fig. 1). Along 46°S small, shallow, warm, saline pockets are evident at Stas 78, 80, and 85. Along all three sections, but particularly along 42 and 46°S, the high-salinity layers of SACW are over-ridden by low-salinity surface water, which the temperature–salinity (T–S) relation (see section 4) indicates is a mixture of SACW and slope water. The thin, low-salinity surface layer does not seem to eliminate the sea-surface temperature signature of SACW water, which is clearly revealed in the i.r. images. The IGY data (FUGLISTER, 1960), the CATO expedition (REID *et al.*, 1977), and Southern Ocean atlas gridpoint data (GORDON and BAKER, 1981) indicate that the low-salinity lid is commonly found south of 30°S and west of the western slope of the mid-ocean ridge near 19°W (IGY Sta. 5822). The regional distribution of the low-salinity lid is about the same as the distribution of the reduced 12 to 16°C thermal gradient, indicating they probably share a similar circulation pattern, perhaps a restricted re-circulation gyre within the southwestern quarter of the South Atlantic Subtropical Gyre.

The 42 and 46°S sections in the Malvinas Current slope region (west of Sta. 38 along 42°S and west of Sta. 85 along 46°S) show a doming up of the isopleths. This 'ridge', which attains minimum depth at Stas 42 to 43 and 88 for the 42 and 46°S sections, respectively, divides the northward flowing Malvinas Current to the west from a southward return flow to the east. The cyclonic baroclinicity represented by this structure extends into the abyssal depths to 3000 to 4000 m. Satellite i.r. data often show cold surface water of the Malvinas Current turning to the south after confluence with the Brazil Current (LEGECKIS, 1978). This circulation pattern is similar to the slope water–Gulf Stream circulation adjacent to the northeast coast of the United States (WORTHINGTON, 1976).

4. POTENTIAL TEMPERATURE-SALINITY RELATION

SVERDRUP, JOHNSON and FLEMING (1942) presented the T–S expression of the central water masses of the World Ocean. The South Atlantic relation [SVERDRUP *et al.* (1942), Fig. 168] is constructed from seven *Meteor* stations scattered evenly between the equator and 40°S. Guided by the North Atlantic thermocline work of ISELIN (1936, 1939) and by WÜST's (1935) Subantarctic Intermediate Water study, SVERDRUP *et al.* (1942) pointed to the similarity of the vertical T–S relation to the surface water relationship within the Subtropical Convergence between 30 to 40°S, as evidence that the central water structure is derived from the Subtropical Convergence.

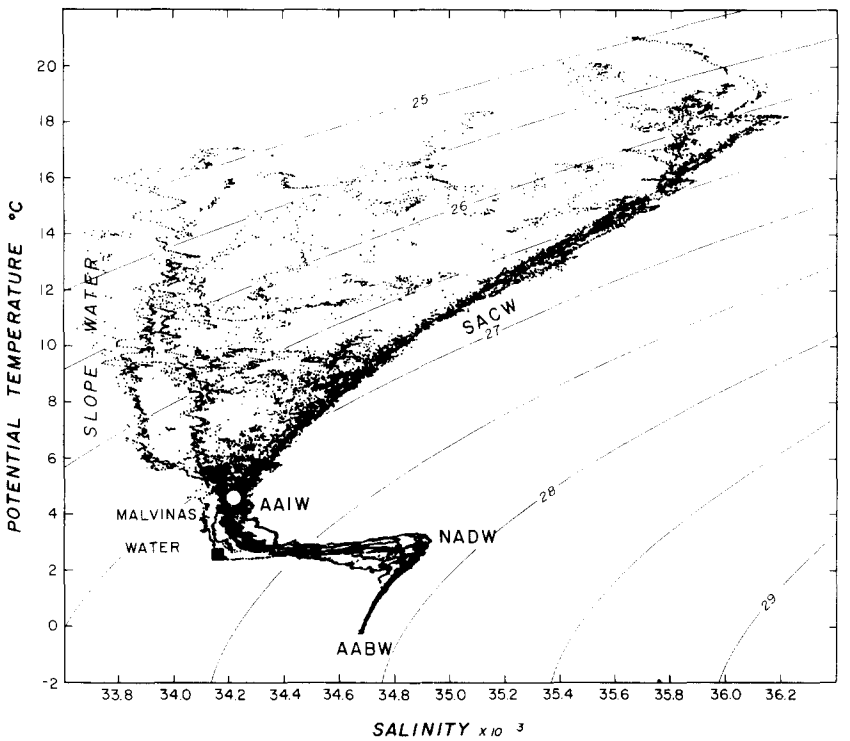

Fig. 5. Group potential T–S scatter diagrams from 12 representative stations. SACW, South Atlantic Central Water; AAIW, Antarctic Intermediate Water; NADW, North Atlantic Deep Water; AABW, Antarctic Bottom Water. The white dot and black square define the warm and cold end points of the Drake Passage isohaline thermocline layer (MOLINELLI, 1978). Sigma-θ lines 25 to 29 are shown.

The T–S curve of the SACW given by SVERDRUP *et al.* (1942) has an envelope width in salinity as measured along isotherms of 0.1×10^{-3} to either side of the central line, from approximately 8 to 13°C. Above 13°C, *Meteor* Sta. 88, in the southwest Atlantic, falls towards high salinity, forcing a greater width of the T–S envelope. The other *Meteor* stations do not show an accelerated salinity increase with higher temperature, so the southwest region presents a positive salinity anomaly above mid-thermocline, relative to the rest of the South Atlantic.

The group potential temperature–salinity relationship, θ–S, of representative *Atlantis II* stations (Fig. 5) indicates the basic water mass structure. There are two regimes, the SACW carried by the Brazil Current and the Subantarctic Waters introduced to the continental margin region by the Malvinas Current.

The slope surface water is a thin layer of low salinity above the thick, nearly isohaline, 2.5 to 5°C Malvinas Water. The slope water must originate along the periphery of the south end of South America, being strongly influenced by continental runoff and flow through the Magellan Straits (KREPPER, 1977).

The Malvinas Water is similar to the isohaline thermocline (Fig. 5; MOLINELLI, 1978) in the northern Drake Passage. The θ–S similarity of the isohaline thermocline and Malvinas

Water clearly indicates that the latter is derived from the former, as expected from the general regional circulation pattern. MOLINELLI (1978) suggested that the Drake Passage isohaline thermocline is induced by isopycnal transfer of Antarctic surface water across the polar front zone into the subantarctic zone, with the top of the isohaline thermocline layer defined by the coldest variety of subantarctic mode water of the southeast Pacific Ocean discussed by MCCARTNEY (1977). This is consistent with WÜST's (1935) assessment that the Antarctic Intermediate Water θ–S structure is a reflection of the north–south surface water θ–S relation across the formation region. The similar subthermocline θ–S structure at the AAIW indicates that the isohaline thermocline–Malvinas Water stratum spreads below the SACW stratification. The slightly higher AAIW salinity relative to the Malvinas Water may be due to mixing with older (re-circulated) subthermocline water (GEORGI, 1979), perhaps aided by relatively rapid downward flux of salt by a salt-finger process discussed in sections 6 and 7.

At the temperatures above 5°C the AAIW nearly isohaline θ–S cluster gives way to the SACW thermocline–halocline θ–S structure. The SACW θ–S curve measured by the *Atlantis II* is similar to the curve by SVERDRUP *et al.* (1942), with the salinity above 12 or 13°C falling along and even beyond the high-salinity limit defined by *Meteor* Sta. 88.

Between the slope and SACW water, roughly above (shallower than) the 27.0 σ_θ level, the group θ–S scatter reflects mixing of slope and SACW. The slope water influence is most intense in the surface layers above the 26.3 σ_θ level. A resilient remnant of SACW intrudes as a salinity maximum into the slope water regime within the 26.6 to 26.8 σ_θ interval. The frequent density compensating thermohaline fine structure within the slope–SACW mixtures indicates the dominance of nearly isopycnal mixing between the slope and SACW water columns. Presumably the tenacious SACW layer in the 26.6 to 26.8 σ_θ interval is a consequence of lack of competition by slope water, which is generally of lower density, or in the case of the Malvinas Water component, of greater density. That the main thermocline oxygen minimum falls in the same density interval may also be a consequence of minimum renewal by isopycnal processes in this density stratum.

The θ–S relation of Sta. 7 (Fig. 6) comparison to a selection of South Atlantic data (IGY, FUGLISTER, 1960; CATO, REID *et al.*, 1977) clearly shows the positive salinity anomaly of up to 0.15×10^{-3} above the 12 to 13°C isotherms, relative to the broader regional SACW θ–S curve. The regional curve (open dashed line in Fig. 6) is defined by the IGY data along 24 and 32°S; it falls along the central axis of the curve by SVERDRUP *et al.* (1942) (adjusted to potential temperature).

The 32°S IGY data points west of Sta. 5822 (19°W) show some high-salinity scatter, particularly those of Sta. 5798, which is within the Brazil Current and close to the *Meteor* Sta. 88 position. The CATO data, which are mostly from west of 20°W between 24 to 42°S, also commonly display high-salinity scatter, relative to the IGY SACW curve.

While Sta. 7 best represents the northern SACW source for the *Atlantis II* SACW extension data, it is interesting that at the 27.0 σ_θ there is an abrupt low-salinity structure, relative to the broad regional SACW θ–S. This low-salinity water is identical to the Malvinas Water. Therefore, the Malvinas Water immediately after confluence with the northern water begins to spread below the thermocline to mix with AAIW, which has been in its subthermocline position for a longer period. Thus, Sta. 7 characteristics, as well as the rest of the *Atlantis II* SACW stations and historical data, indicate the SACW of the southwest Atlantic is anomalously salty above the 12 to 13° isotherms relative to the rest of the South Atlantic SACW θ–S relation. The positive anomaly of salinity seems to be

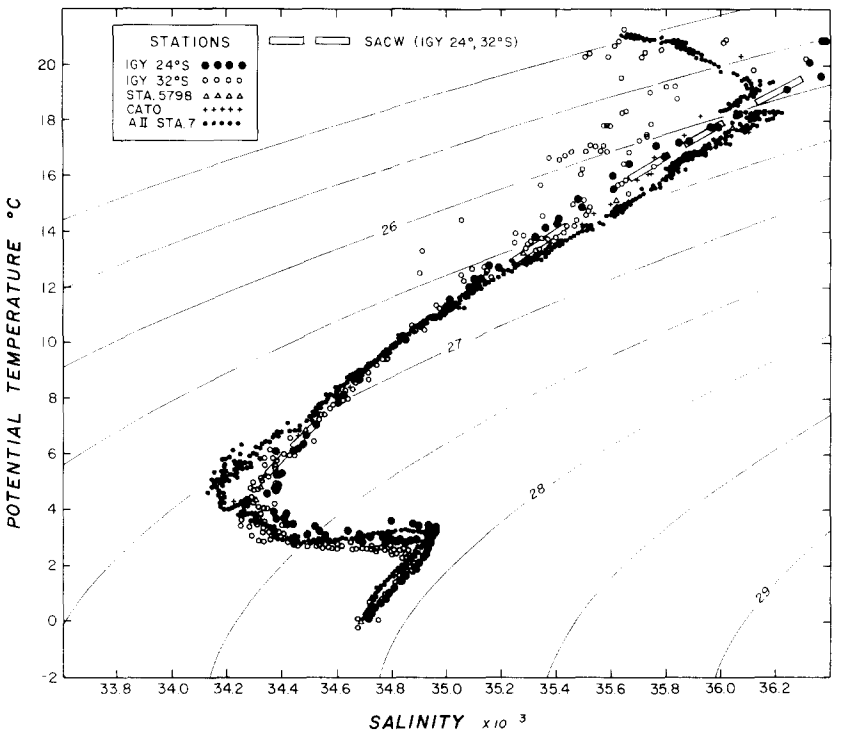

Fig. 6. Potential temperature–salinity (θ–S) relation of Sta. 7 relative to the IGY (International Geophysical Year) and select CATO data. The open dashed line represents the mean characteristics of the South Atlantic Central Water along 24 and 32°S.

associated with the reduced thermal gradient discussed above. The confinement of the positive salinity anomaly and reduced thermal gradient to the southwest Atlantic may be due to the circulation pattern. Reid *et al.* (1977) showed evidence of closed anti-cyclonic circulation in the southwest Atlantic, which becomes better defined and shifts southward in deeper layers. Presumably these features are dissipated or returned poleward in the Brazil Current more rapidly than they are carried north and east within the large-scale Subtropical "Sverdrup" Gyre.

The *Atlantis II* data set can be used to determine the likely source of this anomaly.

5. STRATIFICATION

Station 7 (Fig. 7), which represents the input characteristics to the SACW extension, displays relatively smooth stratification (limited degree of fine structure) within the thermocline–halocline. The lower temperature and salinity gradients above 13°S are clearly evident. Across these features is a broad 5 ml l^{-1} oxygen layer, with a slight minimum near 500 m at the 26.8 σ_θ (9°C isotherm) level. The nearly constant oxygen layer represents a significant gradient in saturation levels. Saturation of 70% occurs near the absolute minimum vs 90 to 100% of full saturation near the top of the thermocline, even though the actual oxygen concentration varies little. Below the absolute oxygen minimum, saturation

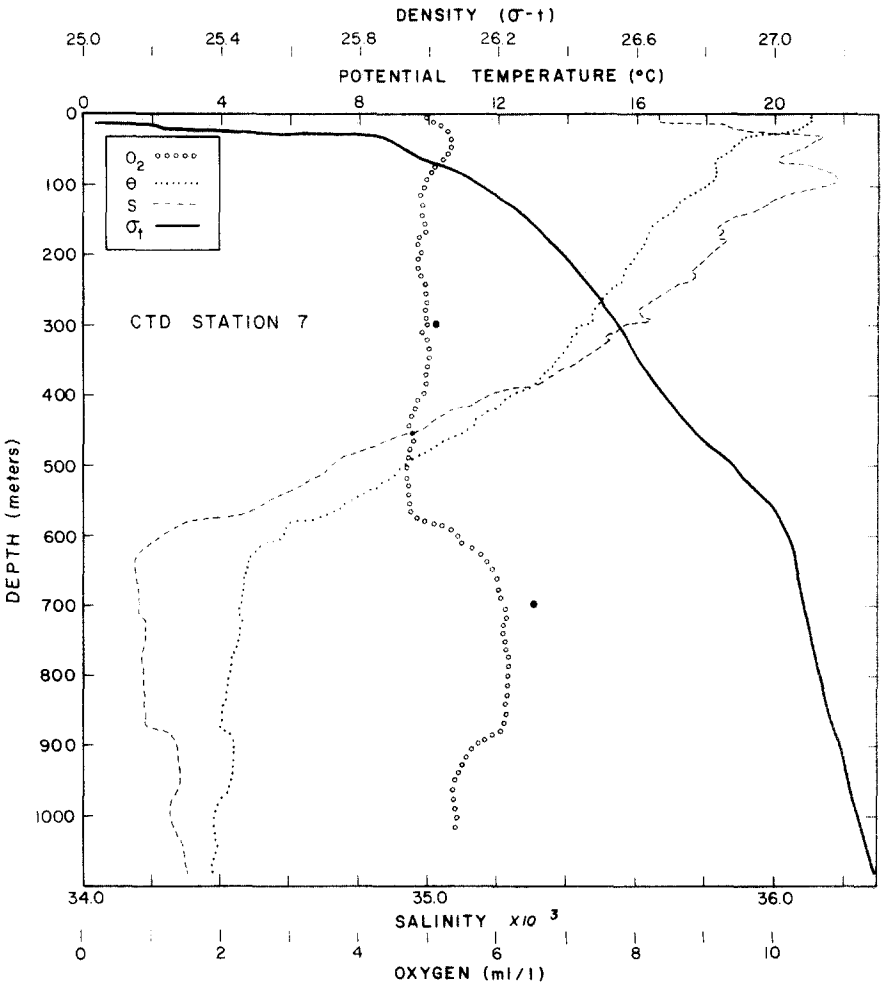

Fig. 7. Potential temperature, salinity, density, and oxygen vs depth trace at Sta. 7. The dots near the oxygen curve represent bottle sample oxygen values taken during the ascent of the CTD. The CTD oxygen sensor is standardized to these bottle samples. As only two bottles were obtained during Sta. 7, the standardization is based on neighboring stations.

increases to about 80 to 90% in the AAIW layer, therefore the thermocline oxygen minimum is much more spectacular in oxygen saturation values.

Hydrographic Sta. 14 (Fig. 8) is within the SACW extension (Figs 3, 4). It has more fine structure than Sta. 7. The largest fine structure feature is the intrusion of a relatively warm, saline (13°C and 35.4×10^{-3}) pycnostad (26.7 σ_θ) layer between 415 and 500 m. Station 16 (Fig. 9) shows a similar feature at 15°C and 35.5×10^{-3} between 250 and 350 m at the 26.35 σ_θ level. Many other stations in the SACW extension along 38°S reveal relatively warm, saline reversals, with usually one or two each station falling into one of four groups (Table 1).

The θ–S relation of Stas 14 and 16 relative to Sta. 7 and the IGY SACW curve (Fig. 10) indicates that the warm, salty intrusions have a positive salinity anomaly of up to 0.25×10^{-3} relative to the IGY curve (as measured along an isotherm). A segment of the

Table 1. Potential temperature groupings by station number of the relatively warm, salty thermocline intrusion observed during R.V. Atlantis II *cruise* 107–3

	15.8°C	15.0°C	13.0°C	12.5°C
Stations	9	11	11	9
	10	12	13	10
	15	13	14	
		16		

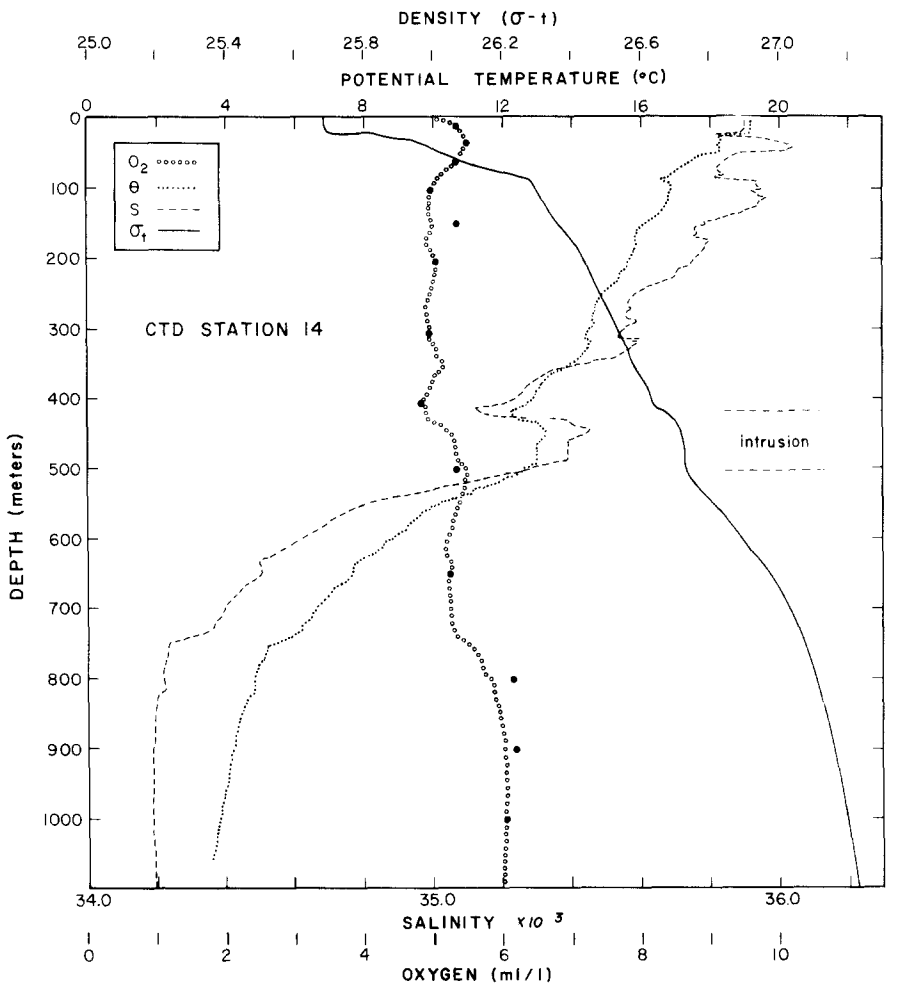

Fig. 8. Potential temperature, salinity, density, and oxygen vs depth traces at Sta. 14. Bottle oxygen values are given by the large solid dots.

Sta. 16 curve, 15 to 16°C, just above the intrusion is identical to the IGY SACW curve, which is indicative of some interaction of the two θ–S regimes.

The potential temperature relations to oxygen and phosphate (Fig. 11) for Stas 14 and 16 indicate that the intrusive layers are higher in oxygen (also see Figs 8 and 9) and lower in

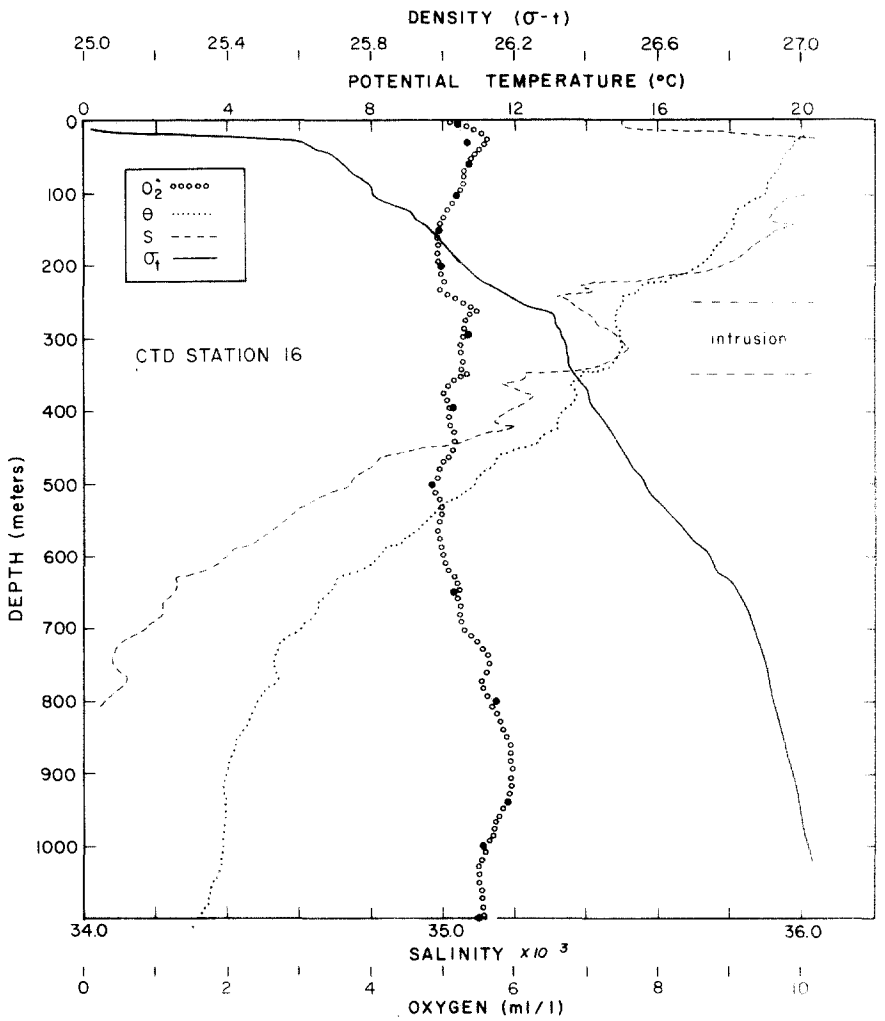

Fig. 9. Potential temperature, salinity, density, and oxygen vs depth traces at Sta. 16. Bottle oxygen values are given by the large solid dots.

phosphate than the Sta. 7 relationships. At Sta. 14 the 13°C intrusion reaches 89% saturation vs 80% above and below the intrusion. The 15°C intrusion at Sta. 16 attains 95% saturation vs 85% above and below. Thus, a significant elevation of oxygen and particularly oxygen saturation levels accompany the positive salinity anomaly intrusions. This feature suggests a recent surface origin of the intrusions.

The origin of the warm, salty intrusions cannot be the low-salinity slope water. The most likely origin is the SACW extension itself. As the warm water is carried poleward by the Brazil Current, thermohaline alterations induced by the winter atmosphere would develop thick mixed layers representing volume maximum of specific θ–S water types, which could then spread into and dominate segments of the stratified thermocline. This process forms McCARTNEY's (1977) Subantarctic Mode Water, the warmest component at the Brazil–Falkland current confluence. Evidence that McCartney is essentially correct is found at

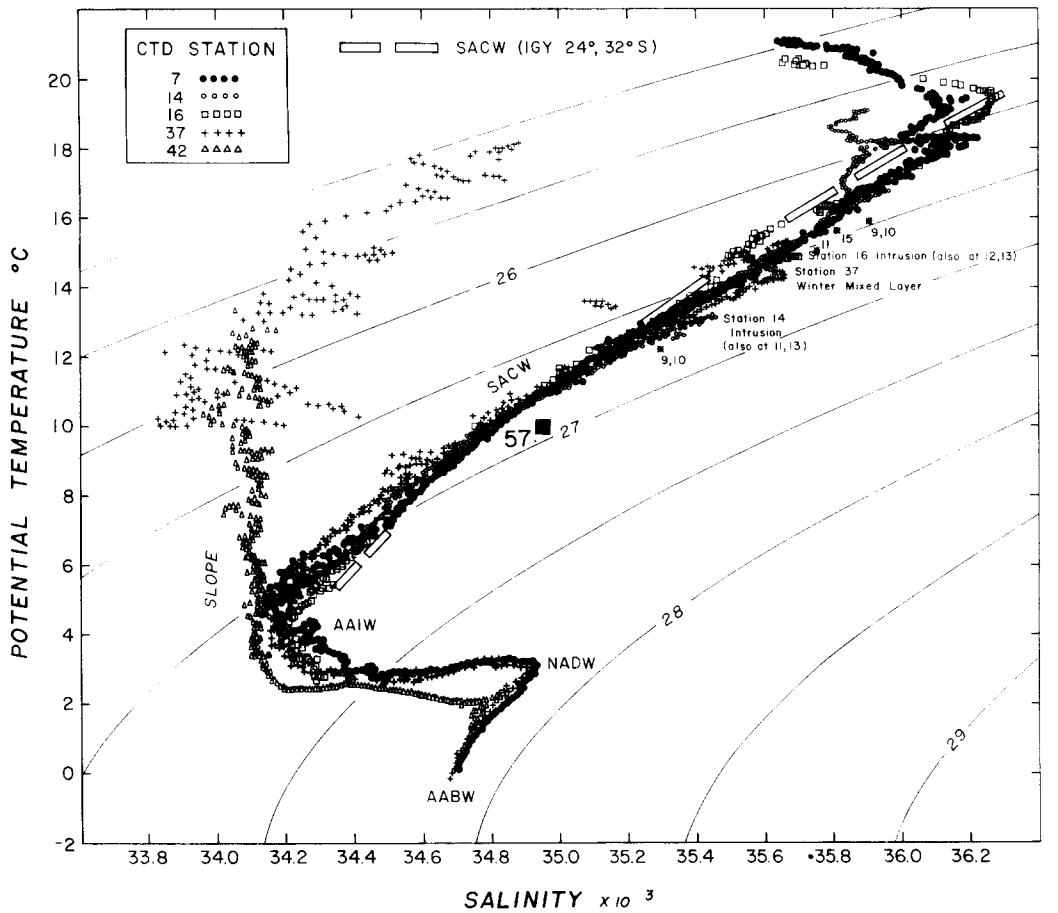

Fig. 10. Potential temperature–salinity (θ–S) relation of Stas 7, 14, 16, 37, and 42. The θ S points of the intrusions for the stations listed in Table 1 are shown as is the mixed layer θ S point of Sta. 57.

Sta. 37 (Figs 10, 11, 12). Station 37 is within a persistent warm meander or eddy within the SACW extension (Figs 1, 3). Below a 50-m 'lid' of low-salinity surface water is a 200-m thick nearly homogeneous layer (particularly in the lower 100 m) of 13 to 14 °C, 35.7×10^{-3} salinity, and 26.65 σ_θ water at 100% oxygen saturation with lower phosphate. This layer also has a positive salinity anomaly relative to the IGY and Sta. 7 θ–S curves.

It is suggested that the Sta. 37 near-surface, warm, salty layer is the remnant of the winter-mixed layer, the low-salinity lid being a post-winter event. Heat flux to the atmosphere is accelerated in the SACW extension (BUNKER, 1980), as the elevated surface temperatures protrude into more subpolar atmospheric conditions. Cooling of the surface water deepens the mixed layer. As the precipitation–evaporation difference in the area is negative [BAUMGARTNER and REICHEL (1975) show a net evaporational loss of up to 20 cm y^{-1}], heat extraction would cause the θ–S point of the mixed layer to migrate towards higher salinity and appear as a positive salinity anomaly relative to the regional θ–S SACW curve. A positive salinity anomaly would occur during cooling even if precipitation were greater than evaporation, as long as the θ–S path of the developing

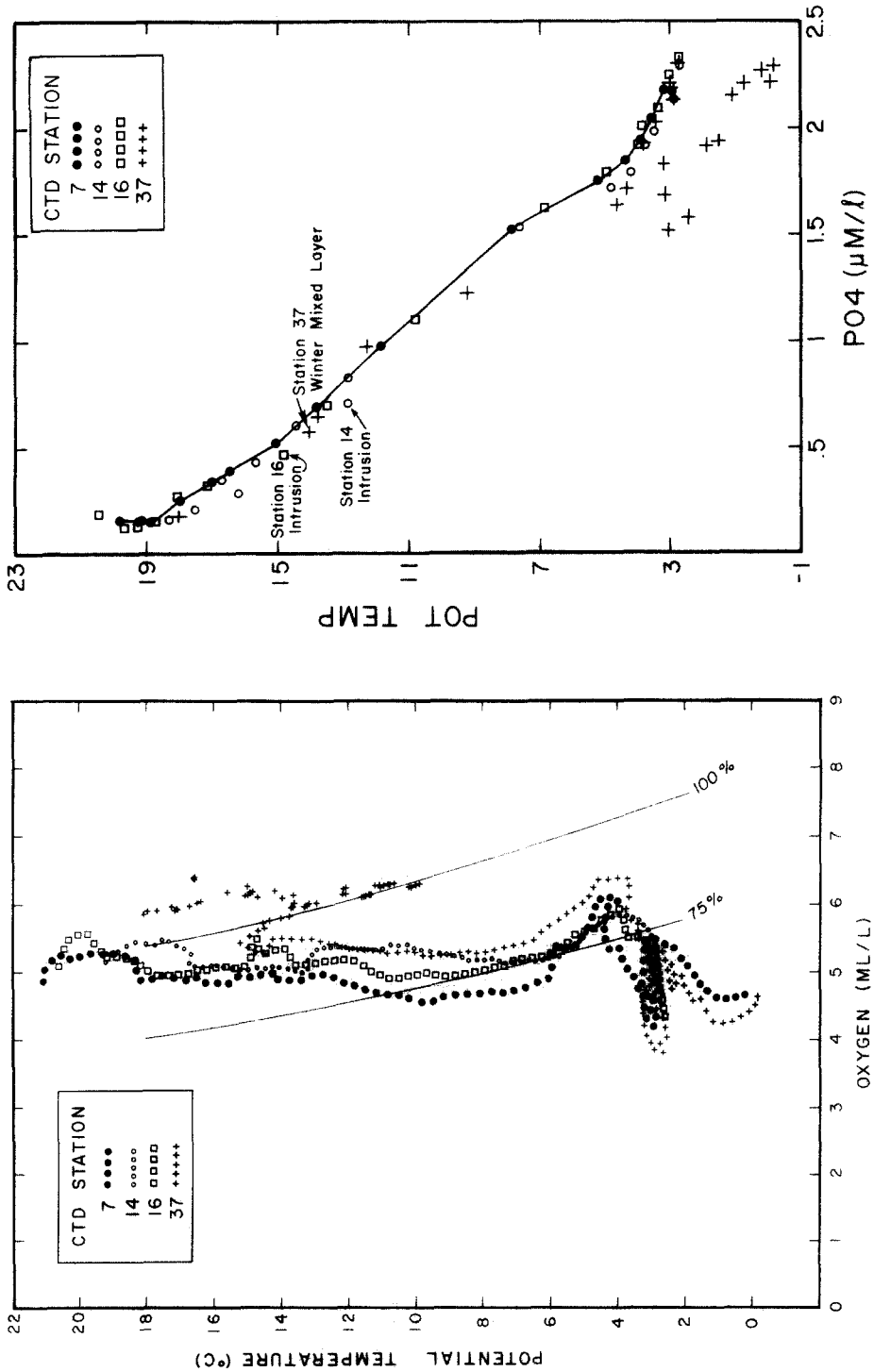

Fig. 11. (a) Potential temperature-oxygen relation for Stas 7, 14, 16, and 37. The 100 and 75% of full saturation lines are given. The symbols represent a trace of the corrected CTD O_2 data. (b) Potential temperature phosphate relation for Stas 7, 14, 16, and 37, obtained from the rosette bottle samples. Station 7 values are connected for reference.

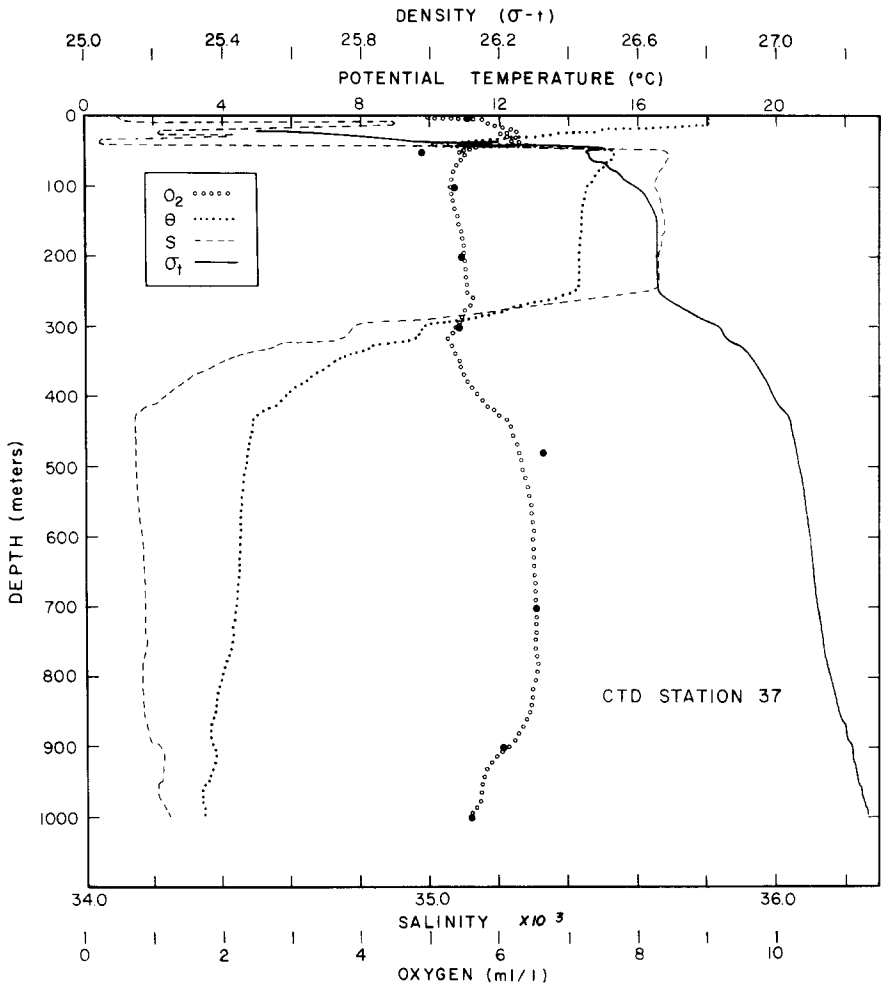

Fig. 12. Potential temperature, salinity, density, and oxygen vs depth trace for Sta. 37. The large solid dots represent bottle oxygen data.

mixed layer were steeper than the regional θ–S curve. This occurs whenever $Q_T/S_0F > \delta\theta/\delta S$, where Q_T is the ocean heat loss, S_0 is the initial mixed-layer salinity, F is the fresh water input, and $\delta\theta/\delta S$ is the slope of the SACW θ–S curve. A net precipitation excess of greater than 0.43 cm day^{-1} (156 cm y^{-1}) is required to prohibit a positive salinity anomaly (using a reasonably conservative winter cooling rate of 50 W m^{-2}).

Excess precipitation over evaporation of such a magnitude along the poleward edges of the World Ocean main thermocline is unlikely. Hence, winter-mixed layers occurring within the central water masses are expected routinely to display a positive salinity anomaly relative to the regional central water T–S curve, as measured along an isotherm.

If altered mixed-layer water, representing a voluminous water type, spreads in a quasi-isopycnal process into the thermocline to the north, it would produce the warm, salty intrusions as observed at Stas 14 and 16. This process effectively transfers upper

thermocline water, which enters the SACW extension with the Brazil Current where heat is removed by the atmosphere, into mid-thermocline depths of the southwest Atlantic and hence is responsible for ventilation of the thermocline, at least to the 12 to 13°C (26.7 σ_θ level).

The complex pattern of warm water within the SACW extension, with its many pockets of warm water, would be expected to form a number of different θ–S modes of mixed-layer water. Therefore, the family of warm, salty intrusions along the 38°S section (Table 1) is a natural consequence of the complex SACW extension spatial pattern. Another aspect of this concept is that the volume and number of mixed-layer water types will depend on the specific SACW extension pattern during the winter months. A more segmented pattern may induce a greater variety of warm, salty intrusions.

The warm, salty intrusions observed along 38°S, relative to Sta. 7 stratification, would eventually mix into the thermocline to induce the broader, more regional positive salinity anomaly of the southwest Atlantic. It is probable that salt fingers play an important role in this regard.

6. THERMOCLINE DENSITY RATIO

Salt-finger activity within temperature stabilized-haline destabilizing stratification, such as the thermocline situation and underside of warm, salty intrusions, may be of significance in driving vertical salt and heat flux (STERN, 1967; LAMBERT and STURGES, 1977). As a consequence of the molecular level of salt diffusivity being two orders of magnitude less than heat conductivity, the effective eddy exchange coefficient for salt becomes larger than the eddy coefficient for heat (SCHMITT and EVANS, 1978). In this way warm, salty layers become progressively cooler, fresher, and less dense (TURNER, 1978; TOOLE and GEORGI, 1981).

The density ratio $R = -\alpha\Delta\theta/\beta\Delta S$ (where α and β are the equation of state coefficients relating density changes to temperature and salinity variation, respectively, and $\Delta\theta/\Delta S$ is the observed slope of the θ–S curve) can be taken as a measure of salt-finger growth rate and probability of being significant. The South Atlantic main thermocline has an R value of about 2 (INGHAM, 1966; also see the Fig. 6 IGY θ–S curve), which is believed to define the upper boundary of R in which salt fingers are important (SCHMITT and EVANS, 1978; SCHMITT, 1979a; also see SCHMITT, preprint). At R values less than 2 rapid salt-finger growth rates increase their probability of occurrence. Curved θ–S relations occur within all of the World Ocean thermoclines (SVERDRUP *et al.*, 1942; INGHAM, 1966). Such a structure immediately places in question the validity of simple thermocline two-point mixing models along the vertical coordinate using the same eddy coefficient for both heat and salt. Curved θ–S regressions suggest the importance of lateral (isopycnal) effects, differences in the eddy coefficients for heat and salt, or both.

The positive salinity anomaly of Sta. 7 (which is representative of the southwest Atlantic as discussed above) decreases the stability ratio above the 12°C isotherm. The R value varies from 1.4 to 1.6, increasing the effectiveness of salt fingers. The undersides of the warm, salty intrusions, such as observed at Sta. 14, have still lower R values, 1.2 to 1.3, making them particularly subject to salt-finger activity.

One of the recognized macro-scale manifestations of salt fingers is step stratification structure (LAMBERT and STURGES, 1977), though it is not clear how to apply fully the laboratory results of double diffusion to the real ocean. Aside from the large and well-

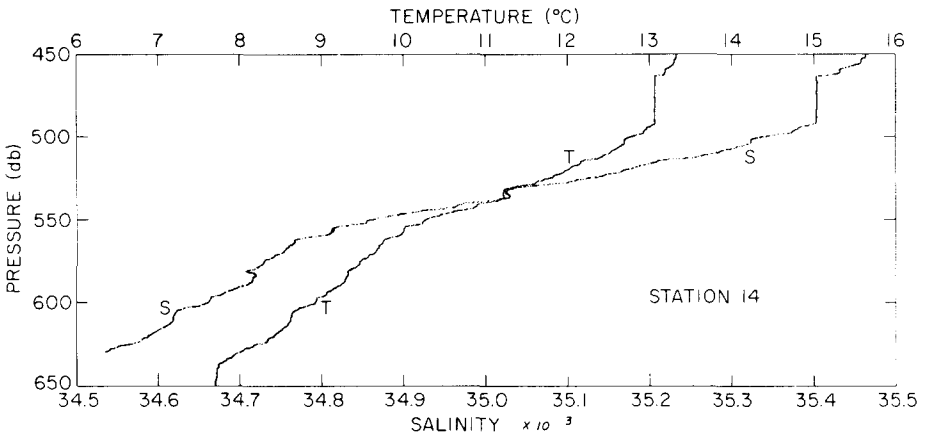

Fig. 13. Expanded temperature and salinity vs depth trace for Sta. 14. The salinity trace displays least spikes for a temperature time constant of 0.2 s.

formed step structure from 463 to 492 m with a salinity discontinuity of 0.03×10^{-3}, the step stratification of Sta. 14 is not well developed (Fig. 13). A small 0.06×10^{-3} salinity step near 540 m and 0.04×10^{-3} steps near 550 to 560 m exist, but they are not sharply defined. A 0.04×10^{-3} salinity step yields a density flux of salt (βF_s) of 1.05×10^{-7} cm s^{-1}, using the relation verified by SCHMITT (1979b):

$$\beta F_s = C(gK_T)^{1/3}(\beta \Delta S)^{4/3}.$$

The salinity flux (F_s) amounts to 1.37×10^{-4} or 4.3 g cm^{-2} y^{-1}. The value of the effective vertical exchange coefficient for salinity is determined, using the F_s value and the large-scale vertical salinity gradient below the Sta. 14 intrusion of 1×10^{-4} cm^{-1}, as 1.37 cm^2 s^{-1}. The corresponding coefficient for heat would be 54% of this value or 0.74 cm^2 s^{-1} using the relation (SCHMITT, 1979b)

$$\frac{\gamma}{R} = \frac{K_{zT}}{K_{zS}},$$

where γ (ratio of density flux of heat to density flux of salt) = 0.7 for $R < 2$ and Sta. 14 R value of 1.3. The effective vertical eddy coefficients are substantially above typical thermocline values, usually taken to be below 1 cm^2 s^{-1} (GARRETT, 1979; GREGG and SANFORD, 1980).

At Sta. 7 there is only a suggestion of steps. However, using the weak steps near 400 m (Fig. 14) with salinity changes of 0.02 to 0.03×10^{-3}, a density flux by salinity and a salinity flux of 0.56×10^{-7} cm s^{-1} and 0.73×10^{-4} or 2.3 g cm^{-2} y^{-1}, respectively, is determined. The effective vertical mixing coefficients for salinity and heat are 1.3 and 0.7, respectively.

The salt flux from the intrusions and regional positive salinity anomalies would lead to attenuation of the feature and increase in the density ratio, forcing an R value approaching 2 (see SCHMITT, preprint). The broad southwest Atlantic positive anomaly represented by Sta. 7 would be reduced by half in about one year, while the warm, salty intrusions would be halved in about 1.5 months.

The excess of evaporation over precipitation in the South Atlantic averages between 80

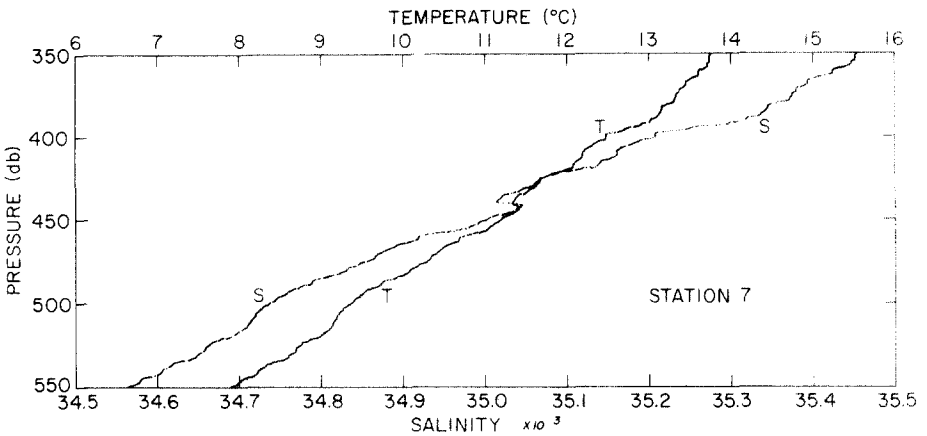

Fig. 14. Expanded temperature and salinity vs depth trace for Sta. 7. The salinity trace displays least spikes for a temperature time constant of 0.2 s.

and 100 cm y^{-1}, while the southwest Atlantic is closer to 20 cm y^{-1} (BAUMGARTNER and REICHEL, 1975). Thus, the downward salt flux induced by the excess evaporation would vary from 0.7 g cm^{-2} y^{-1} in the southwest to 3.5 g cm^{-2} y^{-1} for an oceanic average in the South Atlantic. The salt-finger enhanced salt flux of 2.3 g cm^{-2} y^{-1} at mid-thermocline levels is roughly equivalent to the sea–air exchange flux. Hence, it is suggested that the convective process in the SACW extension transfers the subtropical excess salt to mid-thermocline depths, where it induces a salt-finger active layer. Were it not for the convective deepening, much higher vertical salinity gradients in the upper thermocline would be required to maintain a steady-state salinity balance. The downward salt flux balances the low-salinity AAIW (LAMBERT and STURGES, 1977; SCHMITT, 1979).

7. SOUTHERN SACW EXTENSION

Stratification at the southern end of the warm SACW extension is represented by Stas 54 to 60 (Fig. 3). These stations reveal a thick, nearly homogeneous warm, saline layer in the 100- to 200-m interval. Station 57 is the best example (Fig. 15) with exceptionally well-developed thermohaline steps. The θ–S points of this layer fall to the high-salinity side of the IGY SACW θ–S curve and that of Sta. 7 (Fig. 11). This is taken as evidence that it has had a recent history in the surface mixed layer. However, the temperature of this mixed layer is well below the values for which a northern impact is observed (i.e., it is below the interval of positive salinity anomaly and weakened thermal gradient). This indicates that not all of the thermohaline-altered pockets of SACW spread northward.

The possible fate of the above cold, mixed layers is suggested by the well-formed thermohaline steps as well as the high initial density (26.93 σ_θ) of the mixed layer. The density ratio below the warm, salty feature at Sta. 57 is 1.2.

Homogeneous layers 10 m thick occur in the 225- to 250-m depth interval, with smaller steps at slightly deeper values. The lower part of the warm, salty feature has a 35-m thick, remarkably well-mixed section. The salinity changes at the steps reach 0.06×10^{-3}. This leads to a salt-finger salinity flux of 2.35×10^{-4} or 7.4 g cm^{-2} y^{-1} and an effective vertical

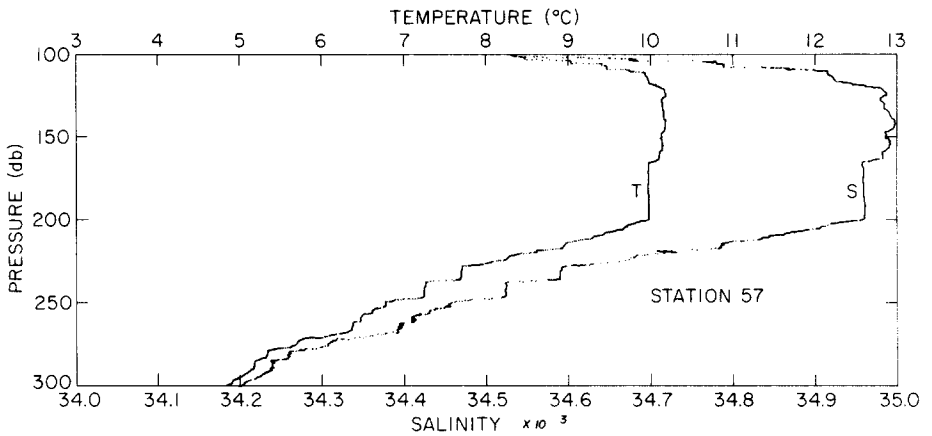

Fig. 15. Expanded temperature and salinity vs depth trace for Sta. 57. The salinity trace displays least spikes for a temperature time constant of 0.2 s.

eddy coefficient for salinity of 2.5 $cm^2\ s^{-1}$ (using the 9.46×10^{-5} large-scale salinity gradient at Sta. 57).

It is suggested that these cold, mixed layers formed at the southern extremes of the SACW extension quickly lose excess salt by salt-finger activity into the AAIW layers, and mix in a nearly isopycnal manner with low-salinity slope water and Malvinas Water. It is possible that thermocline waters in an extreme southern position become isopycnally isolated from the main mass of SACW to the north and hence cannot mix freely into the thermocline.

8. CONCLUSIONS

Thermocline alterations within the poleward extension of the South Atlantic thermocline adjacent to Argentina have two important consequences in regard to water mass renewal.

(1) Relatively salty, deep winter-mixed layers form within pockets of warm water of the SACW extension. These mixed layers, or volume modes in θ–S space, spread northward into the main thermocline, probably by quasi-isopycnal processes. The resultant relatively warm, salty intrusions mix into the thermocline inducing a weakened vertical temperature gradient with a positive salinity anomaly in the 12 to 17°C stratum of the southwest Atlantic thermocline. The process described represents an effective overturning of up to 500 m. It is driven by heat removal from the relatively saline surface water derived from the subtropical excess evaporation region and carried poleward by the Brazil Current.

(2) The positive salinity anomaly generated by injection of winter-mixed layers into the thermocline produces a density ratio minimum at mid-thermocline. This enhances downward salt flux by salt-finger activity and leads to large mid-thermocline vertical mixing coefficients.

The convection transfers excess salt of the near-surface SACW layer to deeper levels, where further vertical transfer by salt fingers carries the salt to deeper layers where it can balance low-salinity Subantarctic inputs into the lower thermocline and subthermocline layers. Along with the salt are higher concentrations of oxygen, which act to ventilate the thermocline.

Similar convective processes may be active along the poleward edges or extensions of other central water masses, particularly where winter period cooling is strong. In the North Pacific, the *Kofu Maru* Sta. 21 (KAWAI, 1972, pp. 284–289), represents late winter conditions (February 1967) with a warm-core eddy shed by the Kuroshio into the "Perturbed Area". The mixed layer, 13.2°C, 34.6×10^{-3} salinity, σ_t 26.06, and 250 m deep, is about 0.1×10^{-3} more saline than the SVERDRUP *et al.* (1942) Northwest Pacific Central Water envelope. Perhaps this eddy combined with mixed layers of other eddies can have an influence on the North Pacific thermocline stratification and renewal. In the South Pacific, ANDREWS and SCULLY-POWER (1976) showed that warm-water eddies of the East Australia Current also develop deep winter-mixed layers (about 300 m thick). HAMON (1970) found that within the East Australia Current region, fine structure with anomalously high salinity, relative to the South Pacific Central Water, occurs in the 13 to 15°C temperature range (see HAMON's Fig. 7).

In the North Atlantic the role of the deep, winter-mixed layer in influencing the thermocline structure is well presented by WORTHINGTON (1972, 1976) in regard to the area of Subtropical Mode Water formation, immediately east of the Gulf Stream. Perhaps the North Atlantic analogy to the South Atlantic situation may involve two additional aspects of North Atlantic thermocline structures. There is the winter alteration of the warm-core eddies shed into the slope region and the thermocline poleward extension east of the Grand Banks. The warm-water eddies develop deep winter-mixed layers (SAUNDERS, 1971; CHENEY, 1976) and would impact a specific density layer of the North Atlantic thermocline when they re-coalesce with the Gulf Stream. It is expected that the winter history of each eddy would differ, hence the mode θ–S characteristics of the mixed layer would display a range rather than a specific value.

The North Atlantic thermocline poleward extension associated with the North Atlantic current east of the Grand Banks (ISELIN, 1936) may have processes identical to that hypothesized for the South Atlantic situation. ISELIN (1936, 1939) showed the surface water θ–S relation of the northwest Atlantic to be similar to the thermocline θ–S relation. He suggested that the thermocline water mass is formed over a broad latitude range at the sea surface, which spreads into the interior thermocline by isopycnal means. The waters east of the Grand Banks form deep winter-mixed layers (see sections presented by WORTHINGTON, 1976) and are enriched in dissolved oxygen relative to the main thermocline to the south (ISELIN, 1939; WORTHINGTON, 1972; CLARKE *et al.*, 1980). Hence, renewal of the North Atlantic thermocline water (at temperatures below 14°C) east of the Grand Banks seems likely and may be analagous to the renewal of the South Atlantic thermocline presented in this study. WORTHINGTON (1972, 1976), ISELIN (1936), and CLARKE *et al.* (1980) presented different circulation schemes for the North Atlantic Current. Worthington believed the thermocline water east of the Grand Banks is replaced from the southeast, while the others believed the replacement is from the southwest.

A general conclusion that can be drawn from this study is that the western boundary current poleward overshoot, which results primarily from the wind-driven circulation, leads to enhanced thermocline ventilation. One wonders if the thermocline consequences of a wind-driven feature acts as a positive, negative, or neutral feedback to the overshoot itself.

Acknowledgements—The collection of high quality hydrographic data was the consequence of the effective work of the cruise participants. ROBERT MCDEVITT of the Woods Hole Oceanographic Institution was responsible for the

operation and maintenance of the WHOI CTD equipment. The nutrient determinations were carried out by the Oregon State University team of WAYNE DICKENSON and J. JENNINGS. Oxygen titrations were done by W. G. METCALF. The Lamont participants were BRUCE HUBER, S. JACOBS, SARAH RENNIE, and JAN SZELAG. The author also acknowledges the dedicated efforts of the officers and crew of *Atlantis II*. The project was funded by Grant OCE 78-23860 of the National Science Foundation. Comments by D. GEORGI, E. KATZ, A. PIOLA, M. MCCARTNEY, and R. SCHMITT are greatly appreciated.

REFERENCES

ANDREWS J. C. and P. SCULLY-POWER (1976) The structure of an East Australian Current anti-cyclonic eddy. *Journal of Physical Oceanography*, **6**, 756–765.

BAUMGARTNER A. and E. REICHEL (1975) *The world water balance*. Elsevier Science Publishers, New York, 179 pp.

BRENNECKE W. (1921) Die ozeanographischen Arbeiten der deutschen Antarktischen Expedition, 1911–1912. *Aus dem Arkiv der Deutschen Seewarte*, **39**, 215 pp.

BUNKER A. F. (1980) Trends of variables and energy fluxes over the Atlantic Ocean from 1948 to 1972. In: *Monthly weather review*, Vol. 108, American Meteorological Society, pp. 720–731.

CHENEY R. E. (1976) A census of rings in the Gulf Stream system. *Nav-oceano Technical Note 3700-44-76*, U.S. Naval Hydrographic Office, Washington, D.C., 10 pp.

CLARKE R. A., H. W. HILL, R. F. REINIGER and B. A. WARREN (1980) Current system south and east of the Grand Banks of Newfoundland. *Journal of Physical Oceanography*, **10**, 25–65.

DEACON G. E. R. (1937) The hydrology of the Southern Ocean. *Discovery Reports*, **15**, 1–124.

DEFANT A. (1961) *Physical oceanography*, Vol. I, Pergamon Press, 729 pp.

FUGLISTER F. C. (1960) Atlantic Ocean Atlas of temperature and salinity profiles and data from the IGY 1957–1958. *Woods Hole Oceanographic Institution Atlas Series I*, Woods Hole, Massachusetts, pp. 1–209.

GARRETT C. (1979) Mixing in the ocean interior. *Dynamics of Atmospheres and Oceans*, Vol. 3, Elsevier Scientific Publishing Company, Amsterdam, pp. 239–265.

GEORGI D. T. (1979) Model properties of Antarctic Intermediate Water in the southeast Pacific and the South Atlantic. *Journal of Physical Oceanography*, **9**, 456–468.

GORDON A. L. and T. N. BAKER (1981) *Southern Ocean Atlas: objective contouring*. Columbia University Press, New York.

GORDON A. L. and E. MOLINELLI (1981) *Southern Ocean Atlas: thermohaline and chemical distributions*. Columbia University Press, New York.

GREGG M. C. and T. B. SANFORD (1980) Signatures of mixing from the Bermuda Slope, the Sargasso Sea and the Gulf Stream. *Journal of Physical Oceanography*, **10**, 105–127.

HAMON B. V. (1970) Western boundary currents in the South Pacific. In: *Scientific exploration of the South Pacific*, WARREN WOOSTER, editor, NAS, Washington, D.C., pp. 50–59.

INGHAM M. C. (1966) The salinity extrema of the World Ocean. Ph.D. Dissertation, Oregon State University, Corvallis, Oregon.

ISELIN C. O'D. (1936) A study of the circulation of the western North Atlantic. *Papers in Physical Oceanography and Meteorology*, **4**, 1–101.

ISELIN C. O'D. (1939) The influence of vertical and lateral turbulence on the characteristics of waters at mid-depths. *Transactions of the American Geophysical Union*, **20**, 414–417.

JAPAN OCEANOGRAPHIC DATA CENTER (1978) *Marine environmental atlas—northwestern Pacific Ocean* II. Japan Hydrographic Association H-602.

JOHNSON W. R. and D. R. NORRIS (1977) A multispectral analysis of the interface between the Brazil and Falkland currents from Skylab. In: *Remote sensing of environment*, Vol. 6, Elsevier, New York, pp. 271–288.

KREPPER C. M. (1977) Difusion del Agua Proviniente del estrecho de Magallanes en las Aguas de la plataforma Continental. *Acta Oceanographica Argentina*, **1**, 49–65.

KAWAI H. (1972) *Hydrography of the Kuroshio Extension*, Chapter 8 of *Kuroshio*, H. STOMMEL and K. YOSHIDA, editors, University of Tokyo Press, 517 pp.

LAMBERT R. B. and W. STURGES (1977) A thermohaline staircase and vertical mixing in the thermocline. *Deep-Sea Research*, **24**, 211–222.

LEGECKIS R. (1978) A survey of worldwide sea surface temperature fronts detected by environmental satellites. *Journal of Geophysical Research*, **83**, 4501–4522.

LUTJEHARMS J. R. E. and D. J. BAKER, JR. (1980) A statistical analysis of the meso-scale dynamics of the Southern Ocean. *Deep-Sea Research*, **27**, 145–159.

MCCARTNEY M. S. (1977) Subantarctic Mode Water. *A voyage of discovery*, M. ANGEL, editor, Pergamon Press, pp. 103–119.

MOLINELLI E. (1978) Isohaline thermoclines in the southeast Pacific Ocean. *Journal of Physical Oceanography*, **8**, 1139–1145.

POND S. and K. BRYAN (1976) Numerical models of the ocean circulation. *Reviews of Geophysics and Space Physics*, **14**, 243–263.

REID J. L., W. D. NOWLIN and W. C. PATZERT (1977) On the characteristics and circulation of the southwest Atlantic Ocean. *Journal of Physical Oceanography*, **7**, 62–91.

SAUNDERS P. M. (1971) Anticyclonic eddies formed from shoreward meanders of the Gulf Stream. *Deep-Sea Research*, **18**, 1207–1220.

SCHMITT R. W. (preprint) Form of the temperature–salinity relationship in the central water: evidence for double-diffusive mixing. Woods Hole Oceanographic Institution, Woods Hole, Massachusetts, submitted to *Journal of Physical Oceanography*.

SCHMITT R. W. (1979a) The growth rate of super-critical salt fingers. *Deep-Sea Research*, **26**, 23–40.

SCHMITT R. W. (1979b) Flux measurements on salt fingers at an interface. *Journal of Marine Research*, **37**, 419–436.

SCHMITT R. W. and D. EVANS (1978) An estimate of the vertical mixing due to salt fingers based on observations in the North Atlantic Central Water. *Journal of Geophysical Research*, **83**, 2913–2919.

SCHROEDER E. H. (1963) North Atlantic temperatures at a depth of 200 meters. Folio 2 of the Marine Environment, AGS, New York, 11 pp., 9 plates.

STANTON B. R. (1973) Circulation along the eastern boundary of the Tasman Sea. In: *Oceanography of the South Pacific*, New Zealand National Commission for UNESCO, Wellington, pp. 141–148.

STERN M. (1967) Lateral mixing of water masses. *Deep-Sea Research*, **14**, 747–753.

SVERDRUP H. U., M. W. JOHNSON and R. H. FLEMING (1942) *The oceans: their physics, chemistry and general biology*. Prentice-Hall, Englewood Cliffs, New Jersey, 1087 pp.

TOOLE J. M. and D. T. GEORGI (1981) On the dynamics and effects of double-diffusively driven intrusions. *Progress in Oceanography*, in press.

TURNER J. S. (1978) Double-diffusive intrusions into a density gradient. *Journal of Geophysical Research*, **83**, 2887–2901.

WINTERFELD T. and H. STOMMEL (1972) *Distribution of stations and properties at standard depths in the Kuroshio area*, Chapter 3 of *Kuroshio*, H. STOMMEL and K. YOSHIDA, editors, University of Tokyo Press, 519 pp.

WORTHINGTON V. (1972) Anticyclogenesis in the oceans as a result of outbreaks of continental polar air. In: *Studies in physical oceanography*, Vol. 1, A. L. GORDON, editor, Gordon and Breach, New York, pp. 169–178.

WORTHINGTON V. (1976) On the North Atlantic circulation. *Johns Hopkins Oceanographic Studies*, Vol. 6, Johns Hopkins University Press, 110 pp.

WÜST G. (1935) Die Stratosphäre des Atlantischen Ozeans. *Wissenschaftlichen Ergebnisse der Deutschen Atlantischen Expedition auf dem Forschungs- und Vermessungschiffe "METEOR"* 1925–1927, Vol. 6, part 1, pp. 109–288.

WYRTKI K. (1962) Geopotential topographies and associated circulation in the western south Pacific Ocean. *Australian Journal of Marine and Freshwater Research*, **13**, 89–105.

WYRTKI K. (1971) *Oceanographic Atlas of the International Indian Ocean Expedition*. National Science Foundation, Washington, D.C., 531 pp.